Residual Analysis of Surface Spectral Radiances Between Instrument Observations and Line-by-Line Calculations

S. A. Clough and P. D. Brown
Atmospheric and Environmental Research, Inc.
Cambridge, Massachusetts

N. E. Miller, J. C. Liljegren and T. R. Shippert
Pacific Northwest Laboratory
Richland, Washington

Introduction

The evaluation and improvement of radiative transfer calculations are essential to attain improved performance of general circulation models (GCMs) for climate change applications. The focus of the study described here is a critical assessment of a radiative transfer experiment conducted under the Department of Energy's Atmospheric Radiation Measurement Program (ARM).

The three principal components of the study are 1) ground-based measurement of the spectral radiances, 2) characterization of the atmospheric state associated with the radiating column, and 3) evaluation of the line-by-line radiative transfer model. The experiment will be continuous (once per hour) and will be conducted over an extended period of time (up to 10 years), important requirements for climate change applications. With respect to global coverage, the first experiment is being conducted in the Southern Great Plains of the United States, with subsequent sites planned for climatologically diverse locations. The initial focus of the experiment is on longwave radiative transfer for clear sky; we plan to extend the approach to include the shortwave and atmospheres with clouds and aerosols. The general concept of this type of study is described by Miller et al. (1994).

Evaluation of the present radiation modeling capability is best achieved by using statistical analyses of the residuals between observed and calculated spectral radiances. Spectral radiances are calculated using the Line by Line Radiative Transfer Model (LBLRTM) (Clough et al. 1991) in conjunction with the HITRAN92 line parameter database (Rothman et al. 1992). Radiance residuals provide a direct indication of all three components of the experiment by physical process.

In the context of the present study, an example of a physical process is the radiance from spectral lines in a specific vibration-rotation band of water vapor. Large spectral residuals associated with water vapor lines could be an indication of problems with the spectroscopy, errors in the observed water vapor profile, errors in the temperature field, or problems with the spectral observations such as the modeling of the instrument function. The methods developed to obtain a quantitative measure of the residuals by physical process are described in this paper. The magnitudes of the means and standard deviations of the residuals provide quantitative measures of the radiative transfer modeling capability over a wide range of atmospheric states. Analyses of these statistical results over time will serve as measures of the capability to observe and model atmospheric radiative transfer and to provide a quantitative indication of improvements in that capability.

Spectral Radiance Observations

Radiance spectra are obtained from the University of Wisconsin Atmospheric Emitted Radiance Interferometer (AERI) at the Cloud and Radiation Testbed (CART) facility of ARM. The AERI is a zenith viewing instrument with a spectral resolution of 0.5 cm^{-1} (unapodized; wavenumber

value to first zero). The spectrum is covered in two bands, 520-1800 cm^{-1} and 1800-3020 cm^{-1}. Radiometric calibrations are done using two high emissivity reference blackbodies (Revercomb et al. 1991). No apodizing function is applied to the data in the interferogram domain other than the rectangular window function, resulting in a sinc scanning function in the spectral domain. The characteristics of the instrument are provided in Table 1. The measured spectral radiances have been corrected to account for the effect of the finite field of view.

Definition of the Atmospheric Radiating Column

The atmospheric column is divided into 24 layers, chosen to accurately model the radiative transfer to the surface associated with the molecular species of interest, including ozone. Although the radiance in the zenith at the surface is generally dominated by the lower altitude regime, contributions from higher altitudes for ozone, which is not uniformly mixed, are important. This layering also enables use of the line-by-line results for cooling rate calculations important for other aspects of ARM.

Table 1. AERI instrument characterization.

Spectral Range (cm^{-1}):	
Channel 1	520-1800
Channel 2	1800-3020
Effective Laser Wavenumber (cm^{-1}):	15798.52
Field of Zenith View Half Angle (mr):	50
Spectral Resolution (cm^{-1}): (wavenumber to first zero)	0.5
Noise (670-1400 cm^{-1}) ($W/m^2sr \cdot cm^{-1}$)	<0.2
Blackbody Reference Sources:	
Emissivity	0.99
Temperature, warm (K)	~333.0
Temperature, ambient (K)	~293.0
Interferometer:	BOMEM MB100
Measurement Time (s):	
Total	600
Sky dwell	180
Warm blackbody view	120
Ambient blackbody view	120

Several sources are used to define the atmospheric column. Temperature profiles are currently derived from radiosondes and in the future, will be taken from 915-MHz and 55-MHz radio acoustic sounding systems (RASS). Water vapor profiles are also currently obtained using radiosondes although we anticipate that they will be supplemented by Raman Lidar in the future. Integrated water vapor column amounts are validated using a microwave radiometer. Molecular volume mixing ratio profiles of CO_2, O_3, CH_4, N_2O, CO, O_2, CCl_4, CFC11, and CFC12 are obtained from climatology. Information regarding the ozone volume mixing ratio can be supplemented by ozone sonde observations on a campaign basis and by the application of a high-resolution retrieval algorithm. An important concern with respect to the radiosonde observations, in addition to the issue of accuracy, is that sondes may not adequately represent the radiating column due to spatial and temporal displacement.

Line-by-Line Radiative Transfer

The line-by-line radiative transfer model being used for this study, LBLRTM, is based on the FASCODE line-by-line model (Clough et al. 1981, 1985). The radiative transfer aspect of the code has been substantially rewritten to support operation on vector processor platforms. The radiance algorithm described by Clough et al. (1992) to treat the vertically inhomogeneous atmospheres has been used, resulting in substantially improved accuracy, and the model is directly applicable to longwave cooling rate calculations. A layered atmosphere is used with each layer assumed to be in local thermodynamic equilibrium (LTE) with respect to the absorption in the layer. The spectral lines are optimally sampled at each layer using an algorithm which effectively provides optimal sampling over the line. An accelerated approximation to the Voigt line shape using a linear combination of precalculated functions is applied to all lines at all layers. The line shape calculation extends to 25 cm^{-1} from line center for all lines, and continua consistent with the adopted line shape definition are provided for self and foreign water vapor broadening

(Clough et al. 1989) and for carbon dioxide. The LBLRTM calculations include continua associated with the collision-induced bands of oxygen at 1600 cm^{-1} and nitrogen at 2350 cm^{-1}, line coupling effects associated with carbon dioxide, and radiative effects of the halocarbons using a pressure dependent treatment on the relevant cross sections available from the HITRAN92 database. Version 3 of LBLRTM, which has improved numerical accuracy (0.05%) and updated water vapor continuum coefficients, is currently being used for these calculations.

An interferogram is obtained from the calculated monochromatic radiances using a Fast Fourier Transform. A rectangular window function consistent with that for the instrument is applied in the Fourier domain, and the resulting interferogram is retransformed to provide the desired calculated spectrum. The results are then interpolated to match the spacing of the data. AERI spectra, taken June 21, 1993, at 11:14 GMT, are shown in the top portions of Figures 1 and 2 for channels 1 and 2, respectively. Spectral residuals, shown in the lower portions of Figures 1 and 2, are obtained by subtracting the LBLRTM results from the measured spectra. The atmosphere is defined from a radiosonde released at 11:18 GMT, with temperature and water vapor profiles given in Figure 3. The water column for this case is 2.5 cm H_2O. The spectral residuals of Figure 1 correspond to a calculated downwelling flux at the surface approximately 10 w/m^2 lower than that measured. The sharp spectral features at 667 cm^{-1} and from 1400-1800 cm^{-1} are due to measurement effects associated with strong spectral lines which provide absorption within the instrument and its calibration path.

Spectral Mapping Functions

A spectral mapping has been developed to associate residuals at each spectral element with a specific physical process. The dependence of spectral elements on molecular species for which the relative density is presumed known correlates elemental sensitivity to the column temperature profile, in addition to the spectroscopy of the species itself. Two indices are defined for each spectral element: an indicator of the sensitivity of the element to changes in the column (mapping function Q_1, a measure

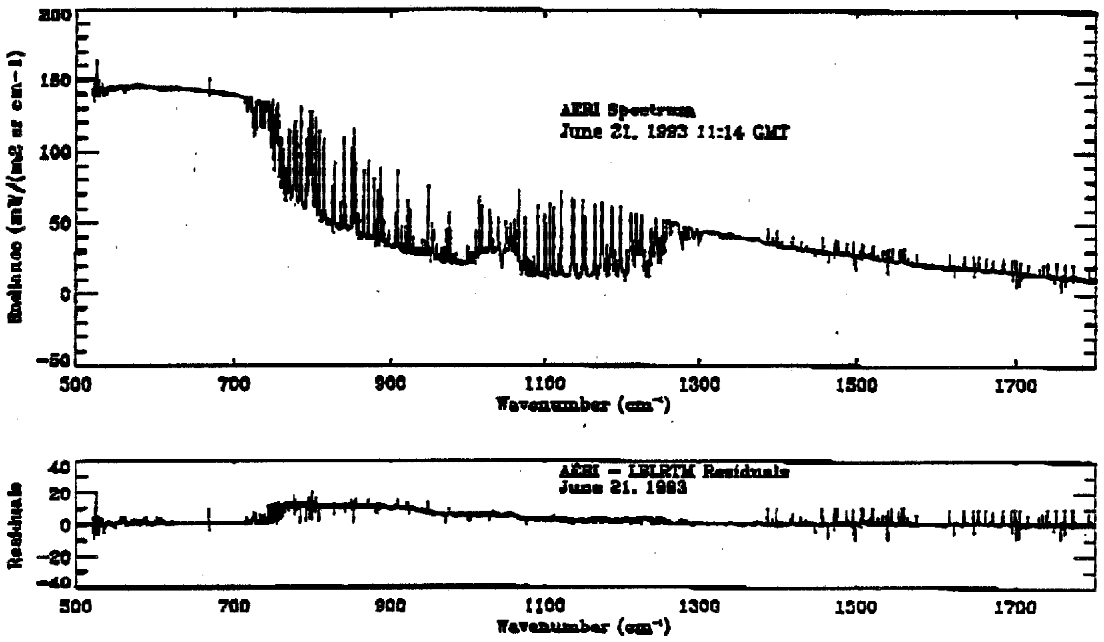

Figure 1. AERI spectrum in the 520-1800 cm^{-1} region, taken June 21, 1993, at 11:14 GMT (top) and the associated residuals with the LBLRTM calculation (bottom, AERI - LBLRTM).

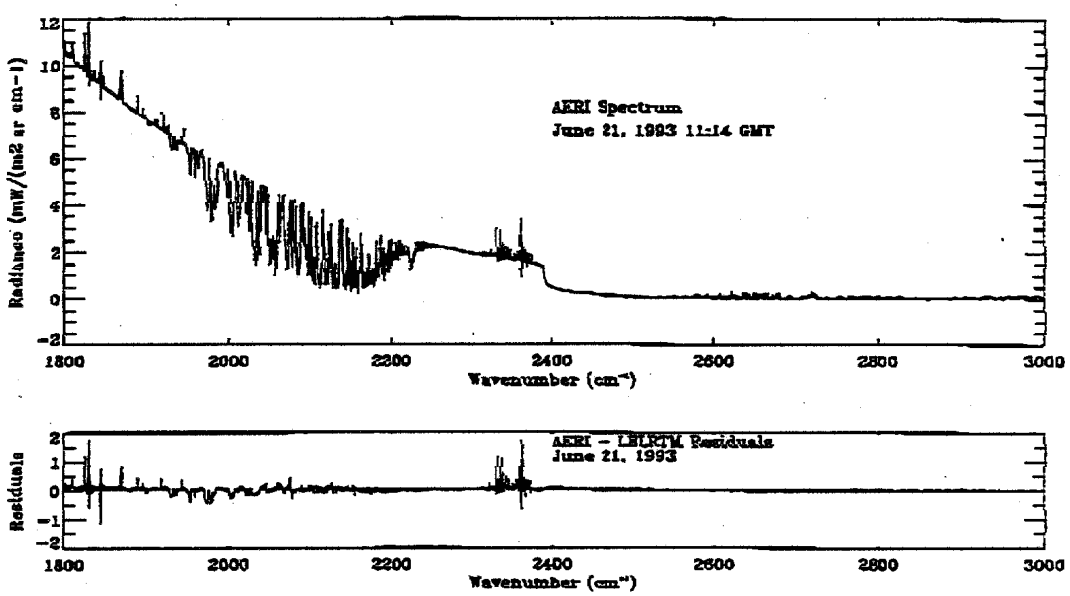

Figure 2. AERI spectrum in the 1800-3000 cm^{-1} region, taken June 21, 1993, at 11:14 GMT (top) and the associated residuals with LBLRTM calculation (bottom, AERI - LBLRTM).

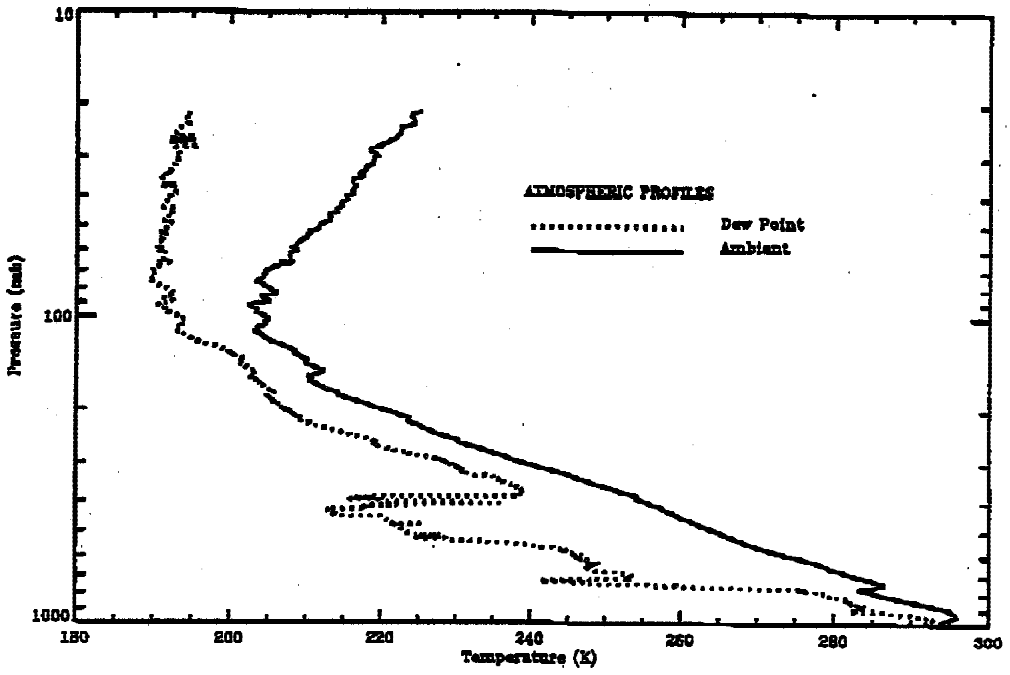

Figure 3. Temperature and water vapor profiles taken from radiosonde launch of June 21, 1993, at 11:18 GMT.

of the atmospheric depth contributing to the radiance), and an indicator of the dominant physical process (mapping function Q_2).

To create a spectral mapping, residuals are obtained between a reference calculation and a series of perturbations of the reference case. The reference calculation uses the midlatitude summer model atmosphere (Anderson et al. 1986) for a single thermally inhomogeneous layer from 0.314 to 2.0 kilometers, used to simplify the computation. The molecules H_2O, CO_2, O_3, O_2, N_2O, CH_4 and CO, as well as the self and foreign water vapor continuum, the carbon dioxide continuum, and the nitrogen continuum, are included in the calculation. The surface temperature is set to 300K, with an average temperature for the layer of 290K. Since ozone is not uniformly mixed, with only 10% contained in the boundary layer, the O_3 column density has been increased tenfold to represent its atmospheric radiative effect more accurately. Subsequent line-by-line calculations are performed with a perturbation in the parameter associated with each physical process. The eleven molecular column densities, the foreign water vapor continuum, the self water vapor continuum, the CO_2 continuum, and the N_2 continuum are separately increased by 1%. The analyses of the differences between the perturbed results and those from the reference calculation provide the information required to generate mappings Q_1 and Q_2.

The calculated brightness temperature in the reference case is an indicator of the extent of the saturation of each spectral point, the degree to which radiance is dominated by the radiating atmosphere in the vicinity of the instrument. Spectral elements with resulting brightness temperatures between 297K and 300K are considered saturated. A value of 0 (insensitive) or 1 (sensitive) has been assigned to Q_1 for each spectral element.

The sensitivity of the radiance to perturbations in physical process is established through the optical depth dependent Planck function used in LBLRTM

$$R = [1 - T][(0.2\tau B_s)/(1 + 0.2\tau) + \bar{B}/(1 + 0.2\tau)] \quad (1)$$

where

R is the layer radiance
τ is the layer optical depth
B_s is the Planck function appropriate to the surface boundary
$\bar{B}$ is the Planck function corresponding to the mean layer temperature
T is the layer transmittance.

The equivalent brightness temperature is used to establish the effect of a species perturbation upon a given spectral element. This is the case even for those spectral elements which are near saturation. A sensitivity function $X(m,\nu)$

$$X(m,\nu) = (T(m,\nu)-T(0,\nu))/(305-T(0,\nu))$$

is defined to determine the physical process sensitivity at each spectral element, where $T(m,\nu)$ is the calculated brightness temperature for process m at wavenumber ν and $T(0,\nu)$ is the reference case brightness temperature at wavenumber ν. The numerator measures the direct sensitivity of the brightness temperature to process perturbation, while the denominator amplifies small changes near saturation relative to the higher sensitivity in less saturated regions. Importantly, X provides a measurement of sensitivity that is independent of wavenumber. The reference number of the perturbed species with the largest value of X has been assigned to Q_2 for each spectral point. Figure 4 shows the reference brightness temperature and the X function for water vapor and carbon dioxide. An unavoidable limitation, particularly with respect to the variability of water vapor, is that the mapping is dependent upon the reference atmosphere chosen.

The oscillatory behavior associated with the sinc instrument function introduces ringing into the spectrum at specific spectral elements. This ringing has an adverse effect upon the sensitivity determination and the selection of a dominant species. To assess the effect of this issue, a Gaussian instrument function with the same resolution has been used. Results of Q_2 for both sets of calculations have been compared, and for those spectral elements which are not in agreement, the value of 0, or "indeterminant," has been assigned to the final Q_2 function. The indeterminant assignment was also made for spectral elements which exhibited strong contributions from more than one physical process. The results of the spectral mapping are shown in Figures 5a and 5b.

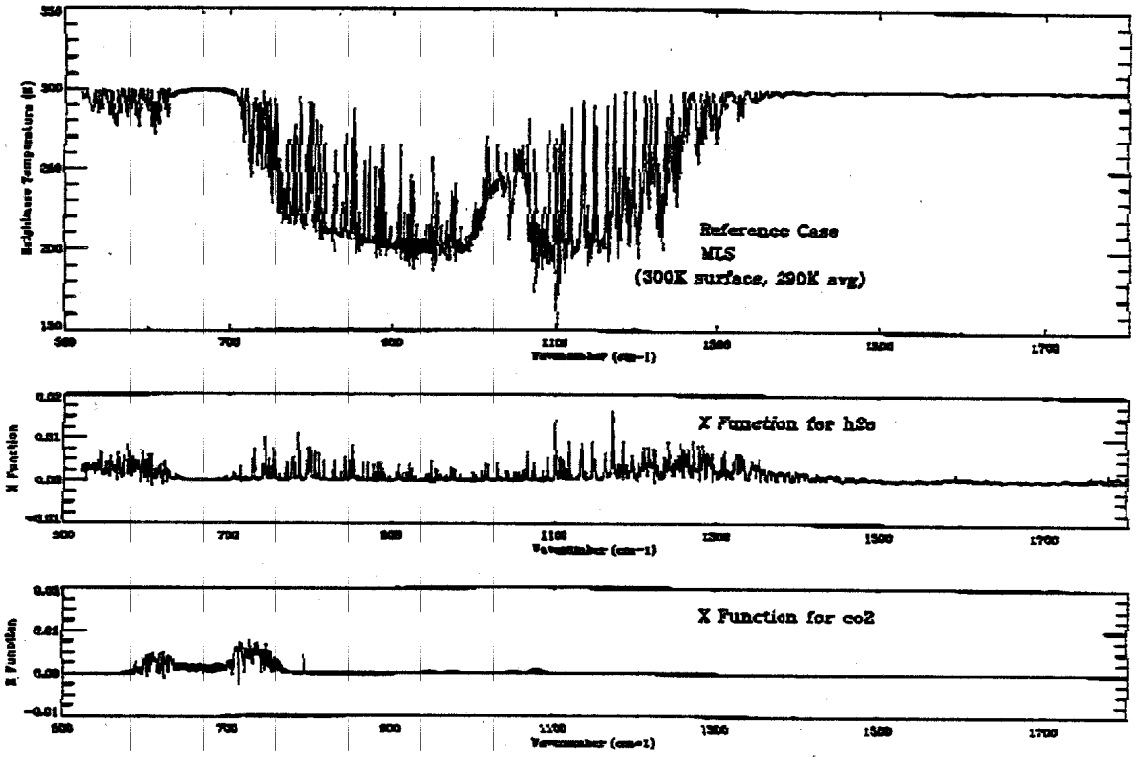

Figure 4. Reference brightness temperature for spectral mapping (top), with X(m,ν) for water vapor lines (middle) and carbon dioxide lines (bottom).

Experiment Products

Statistical analyses are performed upon the spectral residuals between the AERI observed radiances and the LBLRTM calculated radiances with regard to the physical process mapping. To facilitate the analysis of the results, 17 spectral regions demonstrating relatively uniform characteristics with respect to saturation and dominant species have been identified. The criteria used for defining these spectral regions, denoted as "bins," are similar to those used for selecting spectral bands for rapid radiation models used in GCMs. Each bin is defined by a beginning and ending wavenumber, whereby the intersection of any two bins is null and the union of all bins is the spectral range of the experiment. Table 2 lists the bins according to spectral interval, sensitivity, and dominant species.

For each bin, the mean and standard deviation about the mean are obtained by process as well as for all processes combined. This approach enables the differentiation of issues associated with water vapor lines, the water vapor continuum, and carbon dioxide lines (indicating potential errors in the temperature profile or modeling of the instrument function) in spectral regions in which all three processes are active (e.g., the 705-799 cm^{-1} region). In addition, similar statistics are obtained for the broader spectral regions associated with the two AERI measurement regimes and the entire measurement region. The analysis of these means and standard deviations provides the quantitative measure of the quality of the experiment. These results, analyzed over a broad range of atmospheric states, provide a direct indication of the modeling capability and of the physical processes contributing to limitations in that capability.

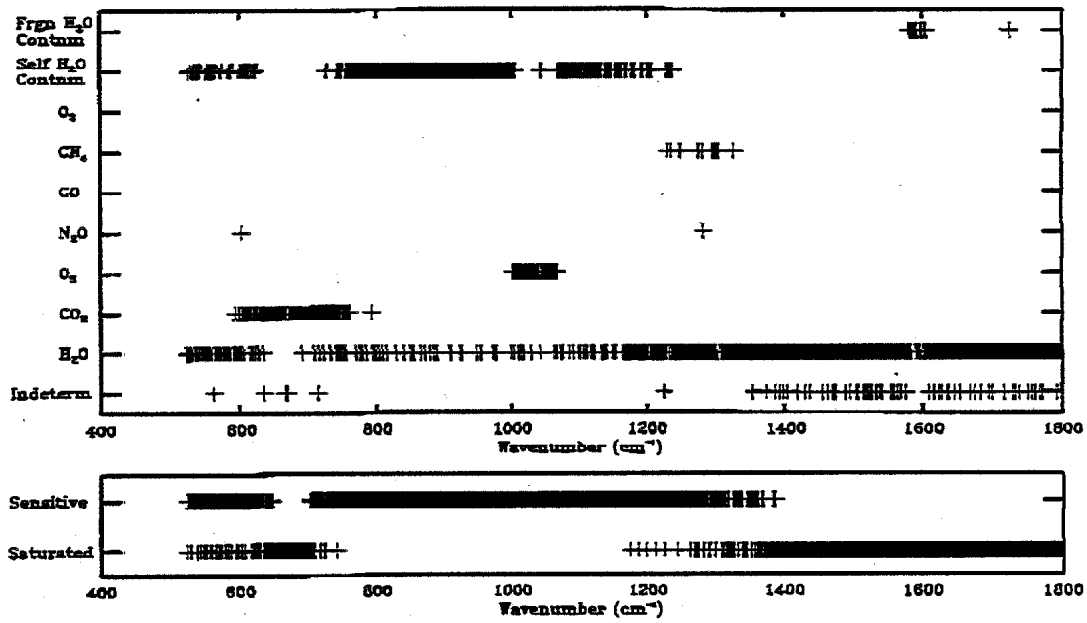

Figure 5a. Final spectral mapping results for the 500-1800 cm^{-1} region.

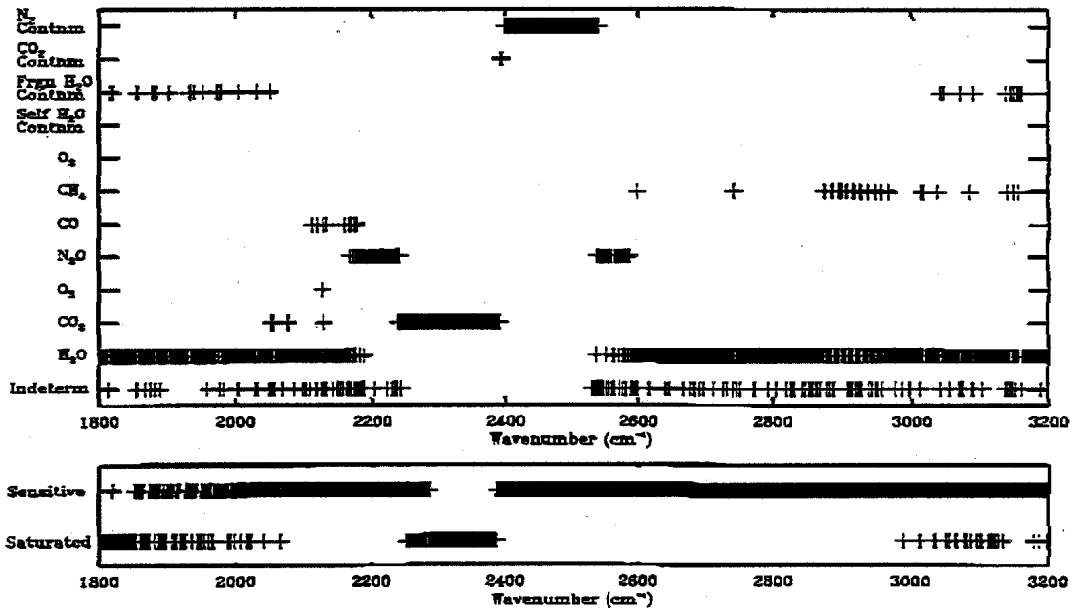

Figure 5b. Final spectral mapping results for the 1800-3200 cm^{-1} region.

Table 2. Bin specification according to spectral interval, sensitivity, and dominant species.

BIN #	Point Interval First	Point Interval Last	Wavenumber Interval First	Wavenumber Interval Last	Sensitivity	Primary Process[a]
AERI Band 1						
1	1	231	520.236802	631.130612		H_2O, sH_2Ocnt, CO_2
2	232	385	631.612759	705.381250	saturated	CO_2, (H_2O)
3	386	579	705.863397	798.917768		CO_2,H_2O,sH_2Ocnt
4	580	999	799.399915	1001.419508		sH_2Ocnt, H_2O
5	1000	1135	1001.901655	1066.991500		O_3, (H_2O)
6	1136	1410	1067.473647	1199.581925		sH_2Ocnt, H_2O
7	1411	1730	1200.064072	1353.868965		H_2O, sH_2Ocnt, (CH_4)
8	1731	2252	1354.351112	1605.549699	saturated	H_2O, fH_2Ocnt
9	2253	2655	1606.031846	1799.854940	saturated	H_2O, (fH_2Ocnt)
AERI Band 2						
10	1	150	1800.337649	1872.177552	saturated	H_2O, (fH_2Ocnt)
11	151	593	1872.659699	2085.768673		H_2O, (fH_2Ocnt, H_2O)
12	594	1009	2086.250820	2286.341825		H_2O, N_2O, CO_2, (CO)
13	1010	1215	2286.823972	2385.664107	saturated	CO_2
14	1216	1656	2386.146254	2598.290934		N_2cnt, N_2O, (CO_2cnt, H_2O)
15	1657	2447	2598.773081	2979.669211		H_2O, (CH_4)
16	2448	2824	2980.151358	3161.438630		H_2O, (CH_4, fH_2Ocnt)
17	2825	3526	3161.920777	3499.905824		H_2O

(a) NOTES:

1. Physical processes in parentheses denote less dominant appearance of process.
2. Molecule names refer to dominant spectral species associated with process.
3. "sH_2Ocnt" refers to self water vapor continuum.
4. "fH_2Ocnt" refers to the foreign water vapor continuum.
5. "N_2cnt" refers to the nitrogen continuum.
6. "CO_2cnt" refers to the carbon dioxide continuum.

Summary

Preliminary statistical analyses provide clear indications of modeling limitations, particularly in the 1000 cm^{-1} window for higher water vapor conditions. Temporal analyses will be performed over longer time scales. Effects over these scales must be considered in the context of changes to the instrument, to atmospheric measurement techniques, and to the radiative transfer model. Assessing modeling capability for less benign atmospheric states such as inversions and fronts is of particular interest. The current results demonstrate the capability to model clear column radiances and to provide insight for future improvements. Initial steps have been taken to extend the current approach to scattering atmospheres and to the shortwave spectral region.

Acknowledgments

We would like to acknowledge highly profitable discussions with W. L. Smith, H. E. Revercomb, and R. O. Knuteson with respect to this research. This research was supported by the U.S. Department of Energy under Grant No. DE-FG02-90ER61064, and by the University of Wisconsin, Subgrant No. G02-7285.

References

Anderson, G. P., S. A. Clough, F. X. Kneizys, J. H. Chetwynd, and E. P. Shettle. 1986. AFGL Atmospheric Constituent Profiles (0-120 km). AFGL-TR-86-0110.

Clough, S. A., M. J. Iacono, and J.-L. Moncet. 1992. Line-by-line calculations of atmospheric fluxes and cooling rates: Application to water vapor. *J. Geophys. Res.* **97**:15761-15785.

Clough, S. A., J. L. Moncet, R. D. Worsham, M. J. Iacono, and A. Bianco. 1991. Radiative transfer model development in support of the Atmospheric Radiation Measurement (ARM) Program. *Proceedings of the Second Atmospheric Radiation Measurement (ARM) Science Team Meeting*, pp. 21-24. CONF-9110336, U.S. Department of Energy, Washington, D.C..

Clough, S. A., F. X. Kneizys, and R. W. Davies. 1989. Line shape and the water vapor continuum. *Atmos. Res*. **23**:229-241.

Clough, S. A., F. X. Kneizys, E. P. Shettle, and G. P. Anderson. 1985. Atmospheric radiance and transmittance. *Proc. of the Sixth Conference on Atmospheric Radiation*. pp. 141-144.

Clough, S. A., F. X. Kneizys, L. S. Rothman, and W. O. Gallery. 1981. Atmospheric spectral transmittance and radiance: FASCOD1B. *Proc. of Soc. Photo. Opt. Instrum. Eng.* **277**:152-166.

Miller, N. E., J. C. Liljegren, T. R. Shippert, S. A. Clough, and P. D. Brown. 1994. Quality measurement experiments within the Atmospheric Radiation Measurement Program. *74th AMS Annual Meeting*, Nashville, Tennessee. American Meteorological Society, Boston, Massachusetts.

Revercomb, H. E., F. A. Best, R. G. Dedecker, T. P. Dirkx, R. A. Herbsleb, R. O. Knuteson, J. F. Short, and W. L. Smith. 1991. High spectral resolution Fourier Transform Infrared (FTIR) instruments for the Atmospheric Radiation Measurement Program: Focus on the Atmospheric Emitted Radiance Interferometer. *Proceedings of the Second Atmospheric Radiation Measurement (ARM) Science Team Meeting*, pp. 121-124. CONF-9110336, U.S. Department of Energy, Washington, D.C.

Rothman, L. S. , R. R. Gamache, R. H. Tipping, C. P. Rinsland, M.A.H. Smith, D. Chris Benner, V. Malathy Devi, J.-M. Flaud, C. Camy-Peyret, A. Perrin, A. Goldman, S. T. Massie, L. R. Brown, and R. A. Toth. 1992. HITRAN molecular database: Edition '92. *J. Quant. Spectrosc. Radiat. Transfer* **48**:469-507.